cmgh
CELLULAR AND MOLECULAR GASTROENTEROLOGY AND HEPATOLOGY

ORIGINAL RESEARCH

Ferroportin Expression in Adipocytes Does Not Contribute to Iron Homeostasis or Metabolic Responses to a High Calorie Diet

Laurence Britton,[1,2,3,4] Lesley-Anne Jaskowski,[1,2] Kim Bridle,[1,2] Eriza Secondes,[4,5] Daniel Wallace,[4,5] Nishreen Santrampurwala,[1,2] Janske Reiling,[1,2,6] Gregory Miller,[2,7] Salvatore Mangiafico,[8] Sofianos Andrikopoulos,[8] V. Nathan Subramaniam,[4,5,§] and Darrell Crawford[1,2,§]

[1]Gallipoli Medical Research Institute, Greenslopes Private Hospital, Greenslopes, Queensland, Australia; [2]The University of Queensland, Herston, Queensland, Australia; [3]Department of Gastroenterology, Princess Alexandra Hospital, Queensland, Australia; [4]QIMR Berghofer Medical Research Institute, Brisbane, Queensland, Australia; [5]Institute of Health and Biomedical Innovation and School of Biomedical Sciences, Queensland University of Technology, Kelvin Grove, Queensland, Australia; [6]Department of Surgery, NUTRIM School of Nutrition and Translational Research in Metabolism, Maastricht University, Maastricht, The Netherlands; [7]Envoi Pathology, Kelvin Grove, Queensland, Australia; [8]Department of Medicine, Austin Hospital University of Melbourne, Heidelberg, Victoria, Australia

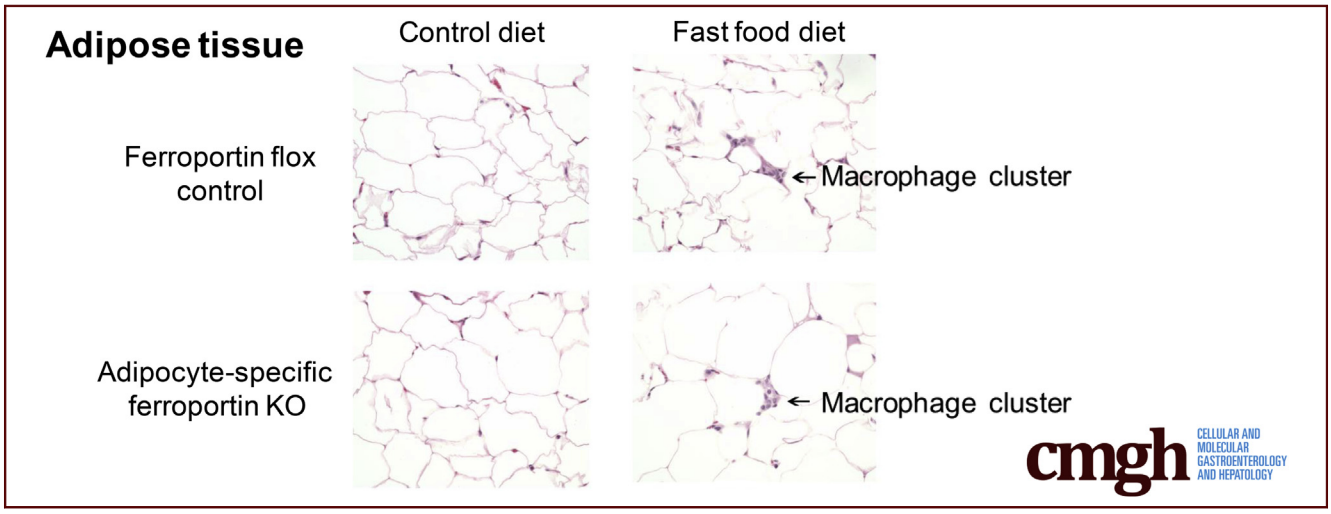

SUMMARY

The iron exporter, ferroportin, has been proposed to have a key role in adipocyte iron homeostasis. Contrary to previous reports, we show that adipocyte-specific ferroportin deletion in mice does not alter adipocyte iron loading, adipokine expression, or glucose homeostasis.

BACKGROUND & AIMS: Iron has an increasingly recognized role in the regulation of adipose tissue function, including the expression of adipokines involved in the pathogenesis of nonalcoholic fatty liver disease. The cellular iron exporter, ferroportin, has been proposed as being a key determinant of adipocyte iron homeostasis.

METHODS: We studied an adipocyte-specific ferroportin (*Fpn1*) knockout mouse model, using an *Adipoq*-Cre recombinase driven *Fpn1* deletion and fed mice according to the fast food diet model of nonalcoholic steatohepatitis.

RESULTS: We showed successful selective deletion of *Fpn1* in adipocytes, but found that this did not lead to increased adipocyte iron stores as measured by atomic absorption spectroscopy or histologically quantified iron granules after staining with 3,3'-diaminobenzidine–enhanced Perls' stain. Mice with adipocyte-specific *Fpn1* deletion did not show dysregulation of adiponectin, leptin, resistin, or retinol-binding protein-4 expression. Similarly, adipocyte-specific *Fpn1* deletion did not affect insulin sensitivity during hyperinsulinemic–euglycemic clamp studies or lead to histologic evidence of increased liver injury. We have shown, however, that the fast food diet model of nonalcoholic steatohepatitis generates an increase in adipose tissue macrophage infiltration with crown-like structures, as seen in human beings, further validating the utility of this model.

CONCLUSIONS: Ferroportin may not be a key determinant of adipocyte iron homeostasis in this knockout model.

Further studies are needed to determine the mechanisms of iron metabolism in adipocytes and adipose tissue. *(Cell Mol Gastroenterol Hepatol 2018;5:319–331; https://doi.org/10.1016/j.jcmgh.2018.01.005)*

Keywords: Iron; Ferroportin; Adipose Tissue; Nonalcoholic Fatty Liver Disease.

Nonalcoholic fatty liver disease (NAFLD) affects approximately 1 billion people worldwide.[1] Many of these individuals develop nonalcoholic steatohepatitis (NASH) and hepatic fibrosis, which can lead to liver failure and hepatocellular carcinoma.[2–4] Treatments that effectively alter the natural history of this disease are lacking and a greater understanding of its pathogenesis is essential to develop such therapies. Dysfunctional adipose tissue has been shown to be central to the pathogenesis of insulin resistance and NAFLD.[5] Adipose tissue serves as the predominant source of liver fat in NAFLD and is the source of adipokines that have significant roles in the regulation of liver injury.[6,7]

Iron is an essential element in cellular metabolism, but also has been implicated in a wide range of human disease.[8] It has been reported that adipocytes within adipose tissue use the same apparatus for iron metabolism as other cell types, such as transferrin receptor 1 (Tfr1), hepcidin, and ferroportin.[9–11] Recent data support a role for iron in the regulation of adipose tissue function. Adipose tissue iron has been proposed as having roles in the pathogenesis of NAFLD as well as type 2 diabetes mellitus.[12,13] Studies have implicated adipose tissue iron in the dysregulation of 4 key adipokines in NAFLD: adiponectin, leptin, resistin, and retinol binding protein-4 (RBP-4).[9,10,14–16] Furthermore, iron has been shown to increase lipolysis in isolated rat adipocytes.[17]

It has been proposed that the cellular iron-exporter ferroportin is a key determinant of adipocyte iron metabolism.[9] Gabrielsen et al[9] showed the down-regulation of adiponectin in response to iron across a range of in vivo and in vitro models. The investigators used an adipocyte protein 2-Cre (AP2-Cre):ferroportin (*Fpn*)$1^{fl/fl}$ model of selective adipocyte ferroportin deletion as a model of adipocyte iron loading. However, results of direct measurement of adipocyte iron were not presented and an iron-loading phenotype was inferred solely on the basis of reduced *Tfr1* messenger RNA (mRNA) quantities.[18] *Tfr1* mRNA quantification remains, at best, an indirect surrogate for iron loading that has not been well validated in adipocytes. Furthermore, the *AP2* gene has been shown to be significantly expressed in other cell types, notably macrophages.[19–21] As such, the importance of ferroportin in adipocyte iron handling requires further validation. The adiponectin (*Adipoq*)-Cre model, which uses a bacterial artificial chromosome transgene Cre recombinase in the promoter region of the adiponectin gene, has been shown to have greater adipocyte specificity than the *AP2*-Cre and is considered to be a superior model of selective adipocyte-specific gene deletion.[20,21]

In this study, we sought to determine whether ferroportin regulates adipocyte iron metabolism by selectively knocking out *Fpn1* in adipocytes using an *Adipoq*-Cre recombinase mouse model. We used the fast food diet model, as described by Charlton et al,[22] as a model for nonalcoholic steatohepatitis in these mice. This article investigates the role of ferroportin in the handling of iron by adipose tissue. In addition, we examined the effect of adipocyte-specific ferroportin deletion on glucose metabolism and liver injury using the fast food diet model of NASH. We also evaluated the utility of the fast food diet model as a model for adipose tissue dysfunction in NASH.

Methods

Experimental Animals

Mice with loxP fragments inserted in exons 6 and 7 of the mouse ferroportin gene ($Fpn1^{fl/fl}$ mice) on a 129/SvEvTac background were a kind gift from Professor Nancy Andrews (Duke University, Durham, NC).[23] $Fpn1^{fl/fl}$ mice were backcrossed for at least 8 generations onto a C57BL/6 background. Male $Fpn1^{fl/fl}$ mice then were crossed with female heterozygous C57BL/6 *Adipoq*-$Cre^{+/-}$ mice expressing Cre recombinase under the control of *Adipoq* (adiponectin gene) promotor regions on a bacterial artificial chromosome transgene (Jackson Laboratory, Bar Harbor, ME).[20] This generated both *Adipoq-Cre:*$Fpn1^{fl/fl}$, adipocyte-specific ferroportin knockout (FKO), and $Fpn1^{fl/fl}$ (Flox) littermate control mice.

After weaning, mice were housed singly. Sixteen-week-old male mice were randomly assigned, using a computerized random allocation sequence generator, to receive either control diet or fast food diet for 25 weeks until the end of the experiment.[22] Control diet mice were provided with drinking water and fast food diet mice were supplied with 42 g/L high-fructose corn syrup (23.1 g/L fructose, 18.9 g/L glucose; Chem-Supply, Gillman, Australia) in the drinking water.[24] Diets were supplied by Specialty Feeds (Glen Forrest, WA, Australia). Mice had ad libitum access to diet and water (control diet) or high-fructose corn syrup in water (fast food diet). The key constituents of the diets are outlined in Table 1.

At 41 weeks of age, mice were weighed. After a 5-hour fast, mice received an intraperitoneal injection of either 0.75 mU/g humulin R insulin (Eli-Lilly, Indianapolis, IN) in sterile 0.9% sodium chloride (0.15 mU/μL; Pfizer, New York), or 5 μL/g 0.9% sodium chloride alone. After 10 minutes, mice were sacrificed as previously described.[25]

Whole liver and epididymal fat pad weights were recorded. Liver and epididymal fat pad samples were fixed in formalin for histology. Liver samples were snap frozen in

§Authors share co-senior authorship.

Abbreviations used in this paper: **AAS, atomic absorption spectroscopy; *Adipoq*, adiponectin; ANOVA, analysis of variance; AUC, area under the curve; bp, base pair; cDNA, complementary DNA; EFP, epididymal fat pad; FKO, ferroportin knockout; Ferroportin Flox, *Fpn1*$^{fl/fl}$; *Fpn1*, ferroportin; *Hamp1*, hepcidin; HIC, hepatic iron concentration; mRNA, messenger RNA; NAFLD, nonalcoholic fatty liver disease; NASH, nonalcoholic steatohepatitis; PCR, polymerase chain reaction; RBP-4, retinol binding protein-4; *Tfr1*, transferrin receptor-1.**

Most current article

2352-345X
https://doi.org/10.1016/j.jcmgh.2018.01.005

Table 1. Major Components of Experimental Diets

Dietary component	Control diet	Fast food diet
Protein, % weight	13.6	17.4
Total fat, % weight	4.0	20
Total digestible carbohydrate, % weight	64.8	48.2
Digestible energy, *MJ/kg*	15.1	18.6
Cholesterol, % weight	0	0.15
Casein (acid), *g/kg*	140	180
Sucrose, *g/kg*	100	341
Clarified butter (ghee), *g/kg*	0	200
Wheat starch, *g/kg*	472	82
Dextrinized starch, *g/kg*	155	0
Iron, *mg/kg*	75	75
High-fructose corn syrup in drinking water, *g/L*	0	42

liquid nitrogen and stored at -80°C. Liver and spleen samples were dried at 110°C for 72 hours for measurement of tissue iron concentration. Blood was collected by cardiac puncture and serum was stored at -80°C. Adipocytes were isolated from epididymal fat pads after collagenase-dispase digestion as previously described and stored at -80°C.[19]

All experiments were performed with approval from the Animal Ethics Committee of the QIMR Berghofer Medical Research Institute and were conducted in accordance with the NHMRC code for the care and use of animals for scientific purposes. Mice were housed in a temperature-controlled environment (23°C) in a 12:12 hour light:dark cycle. All authors had access to the study data and reviewed and approved the final manuscript.

Glucose Tolerance Tests

Glucose tolerance tests were performed 1 week before sacrifice, at 40 weeks of age. After a 5-hour fast, mice were given 1 g/kg glucose via the intraperitoneal route. Tail vein sampling was performed at 0, 15, 30, 60, and 120 minutes and blood glucose was measured using an Accu-Chek Performa II hand-held glucometer (Roche, Basel, Switzerland).

Hyperinsulinemic–Euglycemic Clamp Studies

Hyperinsulinemic–euglycemic clamps were performed as previously described in 6-hour–fasted mice.[26] An initial 2-minute priming dose of insulin (150 mU/kg/min) was followed by constant infusion at a rate of 15 mU/kg/min. Maintenance of euglycemia was achieved by a variable infusion of 25% glucose solution. Steele's steady-state equation was used to calculate glucose turnover.

Tissue Iron Concentration

Hepatic and splenic iron concentrations were measured as previously described.[25] Adipocyte iron concentration was performed on isolated adipocytes by atomic absorption spectroscopy (AAS). Approximately 100 mg of adipocytes for each animal were weighed and then dried at 60°C for 60 hours and 100 μL concentrated nitric acid was added. Samples then were incubated at 60°C for 30 minutes, before dilution 1:5 with zero standard (0.2% nitric acid). Standards over a range of 0–25 μmol/L were prepared using iron pure single element standard 1000 mg/L iron in 2% nitric acid (Perkin Elmer, Waltham, MA). All samples (including standards, quality control, and analytical samples) were diluted further 1:3 with 10 g/L palladium matrix modifier for graphite furnace AAS (Merck Millipore, Darmstadt, Germany). AAS was performed at a wavelength of 372 nm using an AA280Z Zeeman Atomic Absorption Spectrometer

Table 2. Quantitative Reverse-Transcription PCR Primer Sequences (5' to 3')

	Forward primer	Reverse primer
Tfr1	GAGGCAGACCTTGCACTCTT	TGACTGAGATGGCGGAAAC
Fpn1	GCCACTGCGATCACAATCC	TGGAGTTCTGCACACCATTGAT
Hamp1	TTGCGATACCAATGCAGAAG	GGATGTGGCTCTAGGCTATGTT
Adiponectin	GGAGATGCAGGTCTTCTTGG	TCCAGGCTCTCCTTTCCTG
Leptin	GCAGTGCCTATCCAGAAAGTCC	GGAATGAAGTCCAAGCCAGTGAC
Resistin	CATGCCACTGTGTCCCATCGAT	ACTTCCCTCTGGAGGAGACTGT
Rbp-4	TGTAGCCTCCTTTCTCCAGCGA	ACAGGTGCCATCCAGATTCTGC
B2-mg	CTGATACATACGCCTGCAGAGTTAA	ATGAATCTTCAGAGCATCATGAT
Btf-3	TGGCAGCAAACACCTTCACC	AGCTTCAGCCAGTCTCCTTAAAC
Gapdh	TCCTGCACCACCAACTGCTTAGC	GCCTGCTTCACCACCTTCTTGAT
Polr2a	AGCTGGTCCTTCGAATCCGC	CTGATCTGCTCGATACCCTGC
β-actin	CATTGCTGACAGGATGCAGAAGG	TGCTGGAAGGTGGACAGTGAGG
Hprt	GGACTGATTATGGACAGGA	GAGGGCCACAATGTGATG
Hmox1	CACTCTGGAGATGACACCTGAG	GTGTTCCTCTGTCAGCATCACC

Btf3, basic transcription factor-3 gene; *β2-mg*, β2-microglobulin gene; *Gapdh*, glyceraldehyde-3-phosphate dehydrogenase gene; Hmox1, heme oxygenase 1; Hprt, hypoxanthine guanine phosphoribosyl transferase gene; *Polr2a*, RNA polymerase II subunit A gene.

(Varian, Palo Alto, CA) with a GTA 120 Graphite Tube Atomizer (Agilent Technologies, Santa Clara, CA). A Zeeman background correction was used. The final results were expressed per gram wet weight.

RNA Extraction, Real Time Quantitative Polymerase Chain Reaction, and DNA Electrophoresis

RNA was extracted from liver and adipocyte homogenates using Trisure reagent (Bioline, London, UK). Samples were treated with DNase 1 (Invitrogen, Carlsbad, CA) and complementary DNA (cDNA) was synthesized from 1 μg RNA (liver) and 500 ng RNA (adipocytes) using a Sensifast cDNA synthesis kit (Bioline). For quantitative reverse-transcription polymerase chain reaction (PCR), a ViiA7 real-time PCR machine (Invitrogen) with a SensiFAST SYBR Lo-ROX Kit was used (Bioline). Samples underwent thermal cycling as follows: 95°C for 2 minutes, 40 cycles at 95°C for 5 seconds, followed by 63°C for 20 seconds before a melt-curve analysis. Relative mRNA expression was determined by calibration of cycle threshold values to the standard curve of pooled cDNA samples and normalized to the geometric mean of 3 reference genes (basic transcription factor-3, glyceraldehyde-3-phosphate dehydrogenase, and β-2-microglobulin for liver samples, and RNA Polymerase II Subunit A, *β-actin*, and hypoxanthine guanine phosphoribosyl transferase for adipocyte samples). Primer sequences are provided in Table 2.

For confirmation of adipocyte-specific ferroportin knockout, 10 μL of adipocyte *Fpn1* DNA amplification product, created using primers flanking exons 6 and 7 (Table 2) (thermal cycling: 95°C for 2 minutes, 40 cycles at 95°C for 5 seconds, followed by 63°C for 45 seconds) was mixed with 2 μL of 6× DNA loading buffer (New England Biolabs, Ipswich, MA). Samples were electrophoresed at 110 V for 40 minutes in a 1.5% agarose gel (Bioline) mixed with Sybr safe buffer (Invitrogen). The products were visualized on an ImageQuant LAS 500 machine (GE Healthcare Life Sciences, Little Chalfont, UK).

Immunoblotting

A total of 8 μL of 1:1000 mouse serum was electrophoresed on 2% Metaphor Agarose gels (Lonza, Basel, Switzerland) for 75 minutes at 75 V. Protein was transferred onto polyvinylidene fluoride membranes (Bio-Rad, Hercules, CA) over 60 minutes at 100 V. Blocking was performed using 5% skim milk powder. A 1:10,000 dilution of primary antibody against adiponectin (MAB3608; Merck Millipore) was applied to the membranes. A 1:50,000 dilution of goat anti-mouse horseradish peroxidase antibody (Invitrogen) was applied as a secondary antibody. Visualization was performed using a Supersignal West Femto chemiluminescent kit (Thermo Fisher Scientific, Waltham, MA) on an ImageQuant LAS 500 machine (GE Healthcare Life Sciences).

Histologic Assessment and Hepatic Hydroxyproline Assays

Formalin-fixed samples of liver and epididymal fat pad (EFP) were embedded in paraffin. Liver sections were stained with H&E for assessment of steatohepatitis and Sirius Red for assessment of fibrosis. Scoring was performed according to criteria established by Kleiner et al.[27] Further liver sections were stained with Oil Red O and the percentage area stained was measured using ImageJ software, version 2 (National Institutes of Health, Bethesda, MD). EFP sections were stained with H&E and the absolute count of macrophage clusters over 10 high-power fields (×400) was determined. Additional EFP sections were stained with 3,3′-diaminobenzidine–enhanced Perls' stain and eosin counterstain. The average count of iron granules within adipocytes in 5 adjacent high-power fields (×400 magnification) was determined. Small iron granules were counted individually (score, 1), granules filling the whole cell scored 10. All histologic assessments were performed by an expert histopathologist blinded to the study group. Photomicrographs were created using a MicroPublisher 3.3 RTV camera (Q Imaging, Surrey, Canada) and a Biological System Microscope CX41

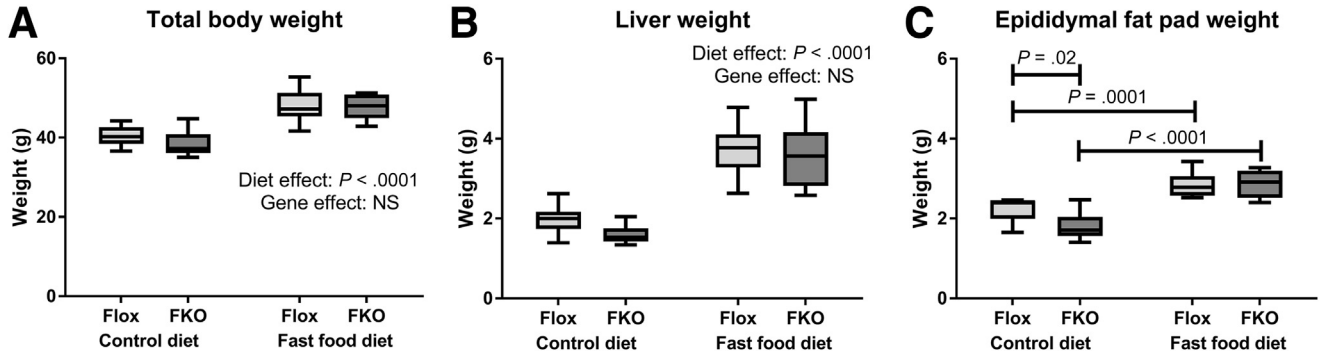

Figure 1. Tissue and body weights. (*A*) Total body weight. Total body weight was increased in animals fed the fast food diet ($P < .0001$), but genotype effect was not significant (NS, 2-way ANOVA). (*B*) Liver weight. Liver weight was increased in animals fed the fast food diet ($P < .0001$), but the gene effect was NS (2-way ANOVA). (*C*) EFP weight. There was a significant interaction between diet and genotype effects ($P = .03$, 2-way ANOVA). Post hoc analysis showed lower EFP weight in FKO mice compared with Flox mice fed the fast food diet ($P = .02$), and increased weight with the fast food diet for both Flox and FKO mice ($P = .0001$ and $P < .0001$ respectively, Sidak's multiple comparisons test); n = 8–12 per group.

(Olympus, Tokyo, Japan). A hepatic hydroxyproline assay was performed as previously described.[28]

Statistical Analysis

Statistical analysis was performed using GraphPad Prism software, version 7.03 (GraphPad, San Diego, CA). Hyperinsulinemic–euglycemic clamp data and glucose concentrations during glucose tolerance tests were analyzed using a 2-tailed Student *t* tests. For liver histology scoring, Mann–Whitney tests were used to compare genotypes for each diet. For all remaining data, 2-way analysis of variance (ANOVA) was used to assess the effect of diet and genotype. If a significant interaction ($P < .05$) was found, Sidak's multiple comparison test was used to compare between genotypes for each diet and between diets for each genotype. In cases in which no interaction was found, *P* values for the diet and genotype effect are indicated. Data presented on box and whisker plots show bars representing the median and interquartile range, with whiskers representing the maximum and minimum values.

Results

Fast Food Diet Was Associated With Increased Body, Liver, and Epididymal Fat Pad Weights

Initial body weight was comparable across all 4 groups (all nonsignificant, Sidak's multiple comparisons test, data not shown). Consistent with the description of the fast food diet model,[22] mice fed with the fast food diet had greater final body weight ($P < .0001$) and liver weight ($P < .0001$, 2-way ANOVA) (Figure 1). EFP weight was higher in both genotypes with the fast food diet ($P = .0001$ Flox mice, $P < .0001$ FKO mice, Sidak's multiple comparisons test) (Figure 1).

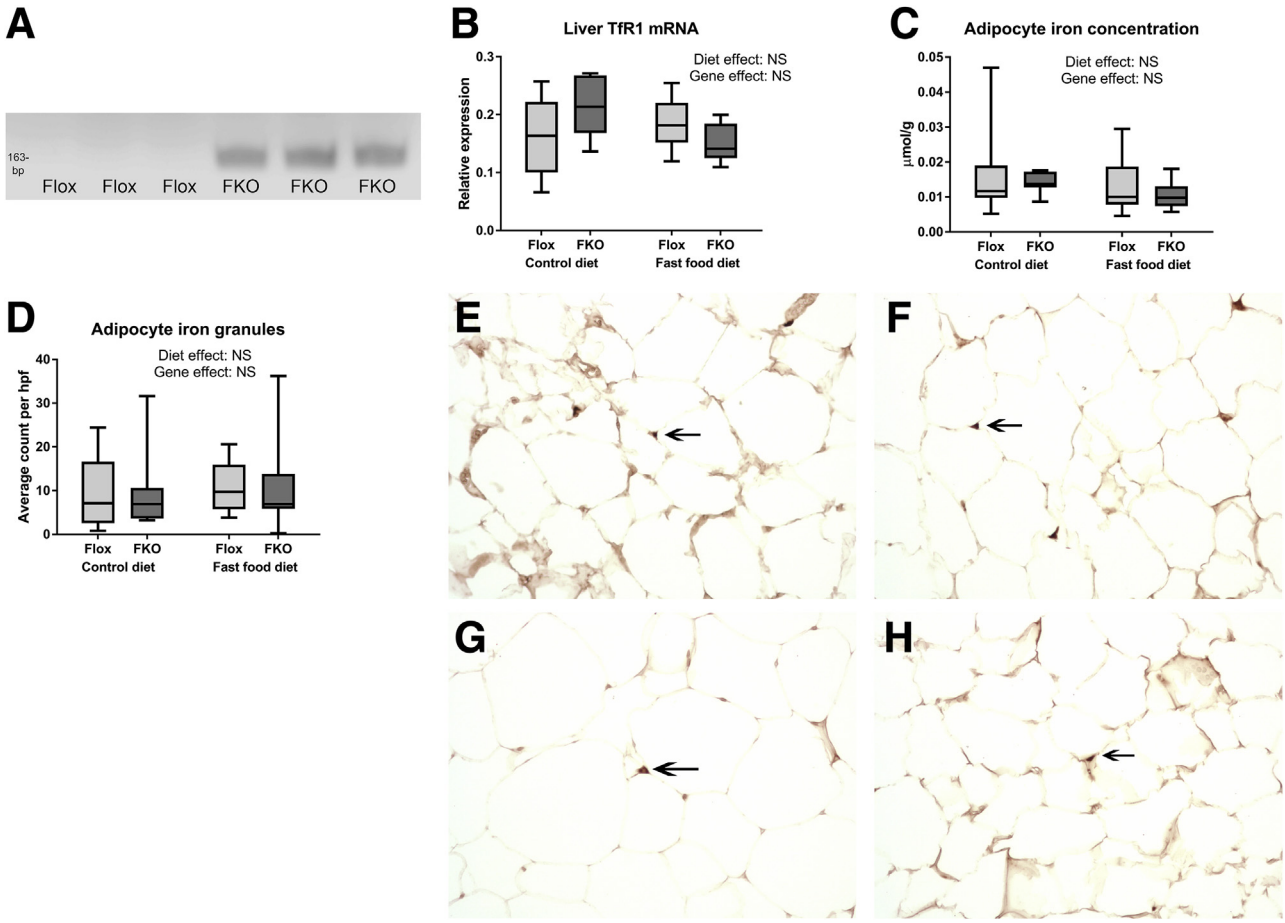

Figure 2. Adipocyte-specific ferroportin knockout does not alter adipocyte iron phenotype. (*A*) Representative DNA electrophoresis blot of adipocyte *Fpn1* reverse-transcription PCR products showing the predicted 163-bp band in adipocytes from FKO but not Flox mice. (*B*) *TfR1* mRNA expression. Diet and genotype effects were both NS (2-way ANOVA; n = 8–12 per group). (*C*) Adipocyte iron concentration. Diet and genotype effects were both NS (2-way ANOVA) (n = 8–12 per group). (*D*) Quantified adipocyte iron granules. Mean count of iron granules in 5 adjacent high-power fields. *Original magnification*: ×400. Diet and genotype effects were both NS (2-way ANOVA; n = 8–12 per group). (*E–H*) Perls' staining of epididymal fat pads. Representative light microscopy sections are shown of eosin and 3,3′-diaminobenzidine–enhanced Perls' stained sections of epididymal fat pads, with *arrows* indicating small iron granules. *Original magnification*: ×400. (*E*) Flox control diet. (*F*) Flox fast food diet. (*G*) FKO control diet. (*H*) FKO fast food diet (n = 7–12 per group).

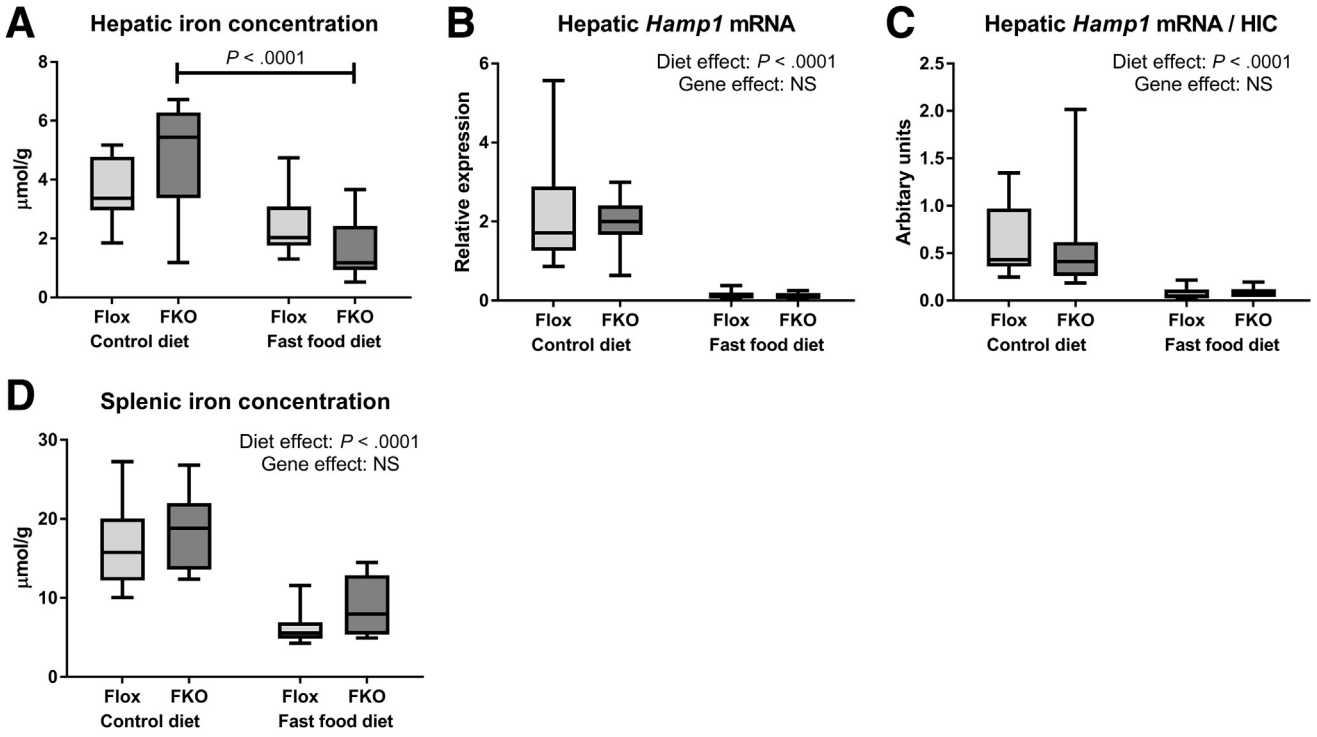

Figure 3. Fast food diet leads to reduced tissue iron concentrations via a hepcidin-independent mechanism. (*A*) HIC. There was a significant interaction between diet and genotype ($P = .03$, 2-way ANOVA). Post hoc analysis showed a significantly lower HIC in FKO animals fed the fast food diet compared with control diet ($P < .0001$, Sidak's multiple comparisons test). (*B*) Hepatic *Hamp1* mRNA expression. Hepatic *Hamp1* mRNA was reduced by fast food diet ($P < .0001$). Genotype effect was NS (2-way ANOVA). (*C*) Hepatic *Hamp1* mRNA/HIC. The hepatic *Hamp1* mRNA/HIC ratio was reduced by the fast food diet ($P < .0001$). Genotype effect was NS (2-way ANOVA). (*D*) Splenic iron concentration. Splenic iron concentration was reduced by the fast food diet ($P < .0001$). Genotype effect was NS (2-way ANOVA; n = 8–12 per group).

FKO Mice Show Successful Selective Adipocyte Knockout of Ferroportin in Adipocytes, but Not in Other Tissues

Fpn1 primers targeting sequences in exons 5 and 8, which flank the *Fpn1* loxP sites, predicted amplification products of 1048 base pairs (bp) for the intact gene and 163 bp for the Cre-recombinase-deleted *Fpn1* gene. DNA electrophoresis of *Fpn1* quantitative reverse-transcription PCR products from isolated adipocytes showed a clear 163-bp band in all 20 samples of FKO mice and no 163-bp band in all 24 samples in Flox mice, indicating adipocyte *Fpn1* deletion in FKO, but not in Flox, mice. A representative gel is shown in Figure 2*A*. In all liver samples, Flox (n = 9) and FKO (n = 8), and all spleen samples, Flox (n = 7) and FKO (n = 14), the 163-bp band was absent whereas a 1048-bp band was present, indicating a lack of Cre recombinase effect in liver and spleen, irrespective of genotype.

Adipocyte-Specific Ferroportin Deletion Does Not Alter Adipocyte Iron Phenotype

All 3 measures of adipocyte iron loading in adipocytes consistently showed no effect of *Fpn1* deletion on iron phenotype (Figure 2*B*–*H*). Quantification of *Tfr1* mRNA as an inversely related surrogate for cellular iron concentration found no genotype effect (NS, 2-way ANOVA) (Figure 2*B*). Similarly, adipocyte iron concentration by atomic absorption spectroscopy was not altered by *Fpn1* deletion (NS, 2-way ANOVA) (Figure 2*C*). Histologic assessment of adipocyte iron granules using 3,3′-diaminobenzidine–enhanced Perls' stain found that iron granule numbers were not increased in FKO mice (NS, 2-way ANOVA) (Figure 2*D*–*H*).

Fast Food Diet Leads to Reduced Tissue Iron Concentrations via a Hepcidin-Independent Mechanism

The hepatic iron concentration (HIC) was reduced by fast food diet in FKO mice ($P < .0001$, Sidak's multiple comparison test) (Figure 3*A*). Reduced HIC with the fast food diet does not appear to be explained by an increase in hepcidin (*Hamp1*) mRNA because *Hamp1* mRNA levels were substantially reduced in fast food diet mice in both genotypes ($P < .0001$, 2-way ANOVA) (Figure 3*B*). Because HIC is an established regulator of hepcidin transcription,[8,29] we normalized *Hamp1* mRNA to HIC and found markedly reduced *Hamp1*/HIC ratios with the fast food diet, likely indicating an appropriate compensatory *Hamp1* response to reduced HIC ($P < .0001$, 2-way ANOVA) (Figure 3*C*). Splenic

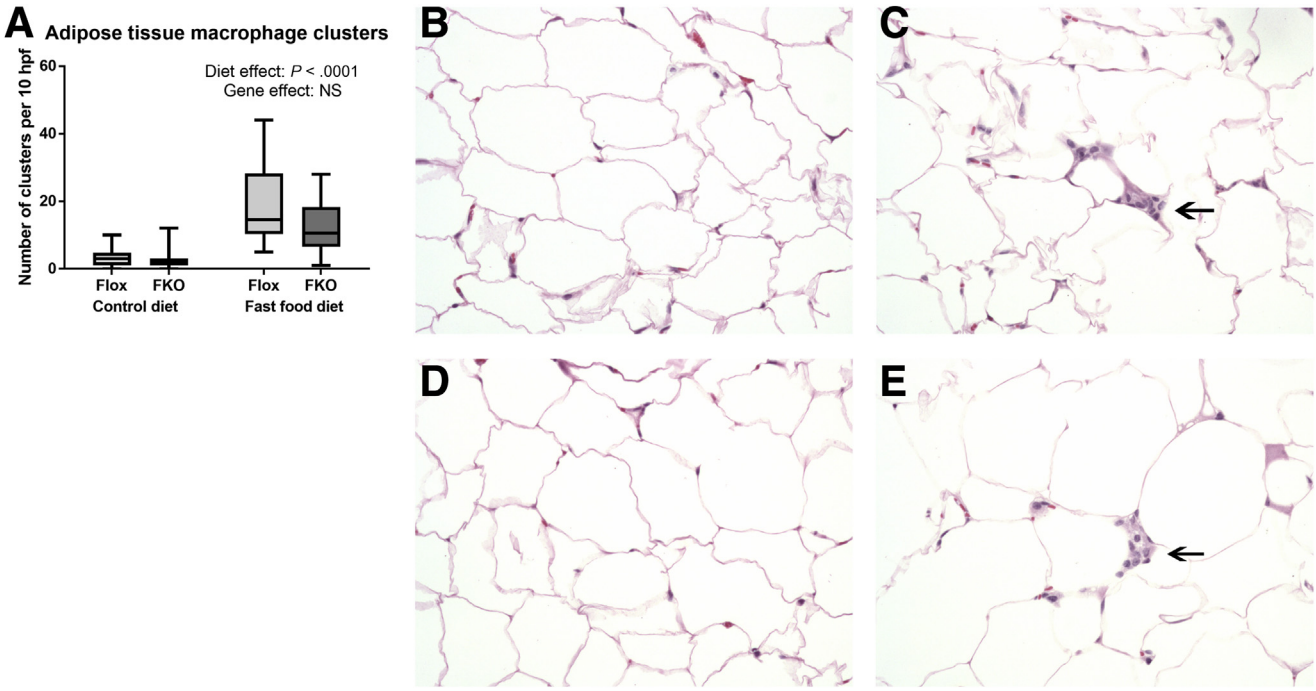

Figure 4. The fast food diet is associated with adipose tissue macrophage accumulation. (*A*) Number of macrophage clusters. Absolute count over 10 high-power fields. Macrophage clusters were increased by the fast food diet ($P < .0001$, 2-way ANOVA). (*B–E*) Light microscopy of representative sections of H&E-stained epididymal fat pads. *Original magnification*: ×400. (*B*) Flox control diet. (*C*) Flox fast food diet. (*D*) FKO control diet. (*E*) FKO fast food diet. (*C* and *E*) *Arrows* indicate examples of macrophage clusters (n = 8–12 per group).

iron concentration also was reduced by fast food diet ($P <$ .0001, 2-way ANOVA) (Figure 3*D*).

The Fast Food Diet Model Is Associated With Adipose Tissue Macrophage Accumulation

Clusters of macrophages, resembling crown-like structures[30] (as indicated by arrows in Figure 4*C* and *E*) frequently were observed in adipose tissue sections from fast food diet–fed mice, but not in their control diet counterparts ($P < .0001$, 2-way ANOVA). *Fpn1* deletion had no effect on the numbers of macrophage clusters (NS, 2-way ANOVA) (Figure 4).

Adipokine Expression Is Unchanged in FKO Mice

There was no effect of *Fpn1* deletion on mRNA quantities of the 4 studied adipokines (adiponectin, leptin, resistin, and RBP-4) in both non–insulin-stimulated (basal, fasted state) animals (Figure 5*A–D*) and in insulin-stimulated animals (Figure 6*A–D*) (all NS, 2-way ANOVA). Fast food diet led to increased *leptin* mRNA quantities in both basal-state and insulin-stimulated animals ($P = .03$ and $P = .01$, respectively, 2-way ANOVA). Fast food diet was associated with reduced *adiponectin* and *resistin* mRNA in insulin-stimulated animals ($P = .0003$ and $P = .01$, respectively, 2-way ANOVA). A reduction in *RBP-4* mRNA was seen in basal-state animals ($P = .01$, 2-way ANOVA) and insulin-stimulated FKO animals ($P = .0008$, Sidak's multiple comparisons test). Total serum adiponectin was unaffected by diet or genotype in basal-state and insulin-stimulated animals (NS in all cases, 2-way ANOVA) (Figure 5*E* and *F*). There were also no significant differences with diet or genotype in basal-state or insulin-stimulated animals for high-molecular-weight adiponectin or high-molecular-weight/total adiponectin ratios (all NS, 2-way ANOVA, data not shown).

Adipocyte-Specific Ferroportin Deletion Does Not Influence Glucose Homeostasis

Intraperitoneal glucose tolerance tests found no significant differences in blood glucose concentrations for both diets at every time point except 120 minutes (Figure 7*A* and *B*). For control diet–fed Flox mice, the mean glucose level at 120 minutes was 16.1 vs 12.8 mmol/L in FKO mice ($P = .02$, Student *t* test). In fast food diet–fed Flox mice, the mean glucose level at 120 minutes was 13.8 vs 11.3 mmol/L in FKO mice ($P = .046$, Student *t* test) (Figure 7*A* and *B*). The area under the curve (AUC) was measured above the minimum glucose value of 7.7 mmol/L as a baseline. Both diet and genotype effects for AUC were nonsignificant (2-way ANOVA, data not shown). For hyperinsulinemic–euglycemic clamp studies performed on fast food diet–fed mice, the mean body weight between the 2 groups was comparable 42.8 g (Flox) vs 43.4 g (FKO) (NS, Student *t* test) (Figure 7*C*). Flox mice had similar basal plasma glucose levels to FKO mice (9.3 vs 9.9 mmol/L) and clamp glucose levels (8.3 vs 8.4 mmol/L) (both NS,

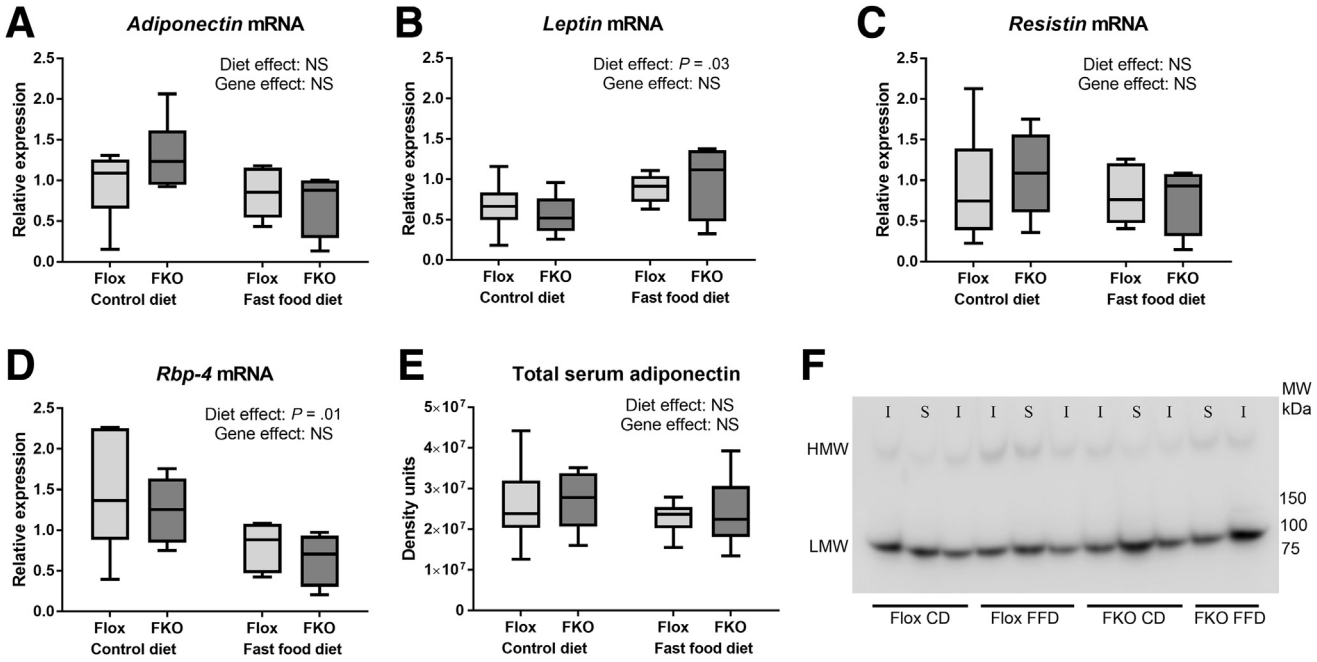

Figure 5. Adipokine expression is unchanged in FKO mice. (*A–D*) Relative mRNA expression of the adipocyte fraction of epididymal fad pads for non–insulin-stimulated animals. (*A*) Adiponectin mRNA. Diet and genotype effects were both NS (2-way ANOVA). (*B*) Leptin mRNA. The fast food diet was associated with increased *Leptin* mRNA ($P = .03$, 2-way ANOVA). (*C*) Resistin mRNA. Diet and genotype effects were both NS (2-way ANOVA). (*D*) *RBP-4* mRNA. The fast food diet was associated with decreased RBP-4 mRNA ($P = .01$, 2-way ANOVA). (*E*) Immunoblotting densitometry of total serum adiponectin (non–insulin-stimulated only is represented here). Diet and genotype effects were both NS (2-way ANOVA; n = 4–6 per group). (*F*) Representative immunoblots of serum adiponectin (presented blot includes both non–insulin- and insulin-stimulated animals as indicated. I, insulin; S, saline (vehicle).

Student *t* test, data not shown). Both groups of mice had substantial increases in mean plasma insulin levels during the clamp studies compared with basal levels (8.3-fold increase in Flox mice [15.7 vs 1.9 ng/mL] and 8.5-fold increase in FKO mice [19.8 vs 2.3 ng/mL]; both $P < .0001$, Student *t* test, data not shown). Overall, there was no evidence of an effect of FKO on glucose homeostasis. The mean glucose infusion rate was 122.9 μmol/min/kg in Flox mice vs 121.7 μmol/min/kg in FKO mice (NS, Student *t* test) (Figure 7*D*). The mean rate of whole-body glucose disappearance was 202.5 μmol/min/kg in Flox mice vs 198.8 μmol/min/kg in FKO mice (NS, Student *t* test) (Figure 7*E*). Under clamp conditions of hyperinsulinemia, both groups, to a similar extent, failed to suppress endogenous glucose production, a measure of hepatic gluconeogenesis, 79.6 μmol/min/kg in Flox mice vs 77.2 μmol/min/kg in FKO mice (NS, Student *t* test) (Figure 7*F*).

Fast Food Diet, but Not Adipocyte-Specific Ferroportin Deletion, Leads to Steatohepatitis

Fast food diet in both genotypes led to steatohepatitis, characterized by severe (grade 3) steatosis with lobular inflammation and prominent hepatocyte ballooning with perisinusoidal and periportal fibrosis. Control diet–fed mice of both genotypes typically had simple steatosis with few balloon cells and an absence of lobular inflammation and hepatic fibrosis. A summary of the histology findings is shown in Table 3 and representative liver sections stained with H&E are shown in Figure 8. In both control diet– and fast food diet–fed animals, there were no significant differences between genotypes for steatosis grade, lobular inflammation, ballooning, or fibrosis (all NS, Mann–Whitney tests). An increased percentage area of steatosis as quantified by Oil Red O staining was found in animals fed a fast food diet ($P = .0001$), whereas there was no difference between Flox and FKO genotypes (NS, both 2-way ANOVA) (Figure 8*E*). Hepatic heme oxygenase-1 mRNA, a marker of oxidative stress response,[31] was increased by the fast food diet ($P < .001$), but unaffected by genotype (NS, both 2-way ANOVA) (Figure 8*F*). Hepatic hydroxyproline was increased significantly by fast food diet ($P < .001$), but not by FKO (NS, 2-way ANOVA) (Figure 8*G*).

Conclusions

In this study, we have shown effective adipocyte-specific ferroportin deletion using an *Adipoq*-Cre recombinase model. Our study shows 3 key findings. First, ferroportin deletion did not result in any alteration of adipocyte iron phenotype, glucose homeostasis, adipokine regulation, or liver injury. Second, we have shown that the fast food diet is associated with reduced hepatic and splenic iron concentrations with a compensatory hepcidin response. Third, we

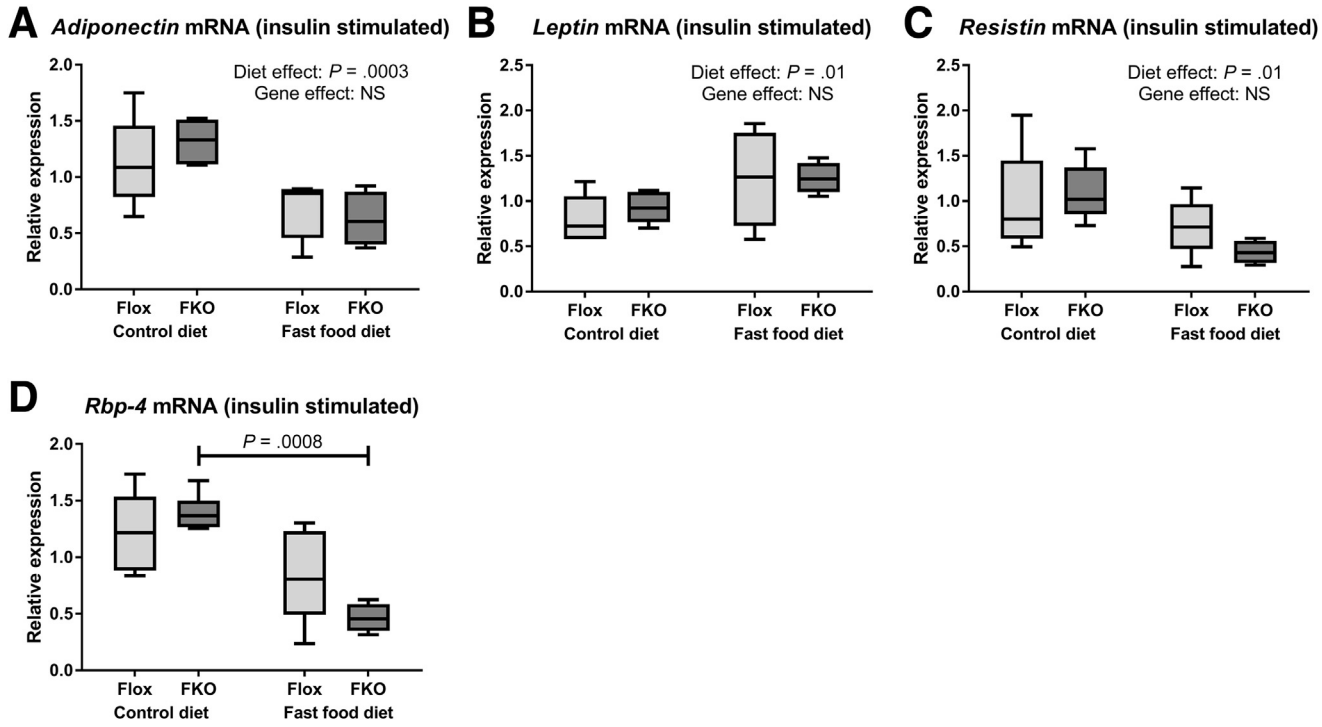

Figure 6. Adipokine expression is unchanged in insulin-stimulated FKO mice. (*A–D*) Relative mRNA expression of the adipocyte fraction of epididymal fad pads (insulin-stimulated state). (*A*) Adiponectin. *Adiponectin* mRNA was reduced by the fast food diet ($P = .0003$, 2-way ANOVA). Genotype effect was NS. (*B*) Leptin. *Leptin* mRNA was increased by the fast food diet ($P = .01$, 2-way ANOVA). Genotype effect was NS. (*C*) Resistin. *Resistin* mRNA was reduced by the fast food diet ($P = .01$, 2-way ANOVA). Genotype effect was NS. (*D*) RBP-4. There was a significant interaction between diet and genotype ($P = .049$). Post hoc analysis found *RBP-4* mRNA was reduced by the fast food diet among FKO animals ($P = .0008$, Sidak's multiple comparisons test). In flox mice the results were NS (n = 4–6 per group).

confirm the fast food diet model's utility as a model for NASH and have identified adipose tissue macrophage infiltration, which further validates this model.

We did not find an adipocyte iron loading phenotype despite successful *Fpn1* deletion in FKO mice. There are several possible explanations for this. First, ferroportin may not have a significant role in adipocyte iron homeostasis. It is not known whether iron importers such as the divalent metal transporter-1 or an unidentified alternative export mechanism may have more important roles in the regulation of iron content in adipocytes. Second, it is possible that the FKO mice would require a longer period of dietary iron loading to generate such a phenotype even in the absence of adipocyte ferroportin. As such, it may be difficult to determine the importance of adipocyte ferroportin to human beings who may accumulate iron over many years.

Gabrielsen et al[9] used the *AP2-Cre* $Fpn^{fl/fl}$ model and reported an iron loading phenotype on the basis of reduced quantities of adipocyte *Tfr1* mRNA leading to reduced adiponectin transcription and insulin resistance. However, data regarding direct iron assay or histologic assessment of iron were not presented. *Tfr1* mRNA quantity is expected to be reduced in iron-loaded cells owing to a negative feedback mechanism involving iron-responsive elements in the *Tfr1* gene 3' untranslated region.[18] However *Tfr1* mRNA is a surrogate that is not well validated as a measure of iron loading and particularly not in adipocytes.

The disparity between the study by Gabrielsen et al[9] and ours could relate to the difference in Cre recombinase site. In addition to its expression in adipocytes, the *AP2-Cre* has been reported to have some degree of expression in macrophages.[19–21] Although altered *Fpn1* mRNA quantities were not seen in splenic extracts by Gabrielsen et al,[9] the *Adipoq-Cre* has been regarded as a more specific Cre recombinase for adipocytes.[21] Differences between the 2 studies also may relate to a difference in mouse strain. The strain was reported as either "129/SvEvTac or C57BL6" by Gabrielsen et al.[9] Regardless, it appears that if Cre-lox models of adipocyte ferroportin deletion are to be used as models of adipocyte iron loading, then the iron-loading phenotype needs to be shown more clearly.

Glucose homeostasis was assessed in this study using intraperitoneal glucose tolerance tests and hyperinsulinemic–euglycemic clamp studies. FKO mice had lower blood glucose concentrations at the 120-minute time point, but not at other time points or on the AUC analysis, suggesting that the significance of this result in isolation is doubtful, particularly given the lack of observed change in iron phenotype. Glucose infusion rate and other measures in the clamp studies found no difference between genotypes,

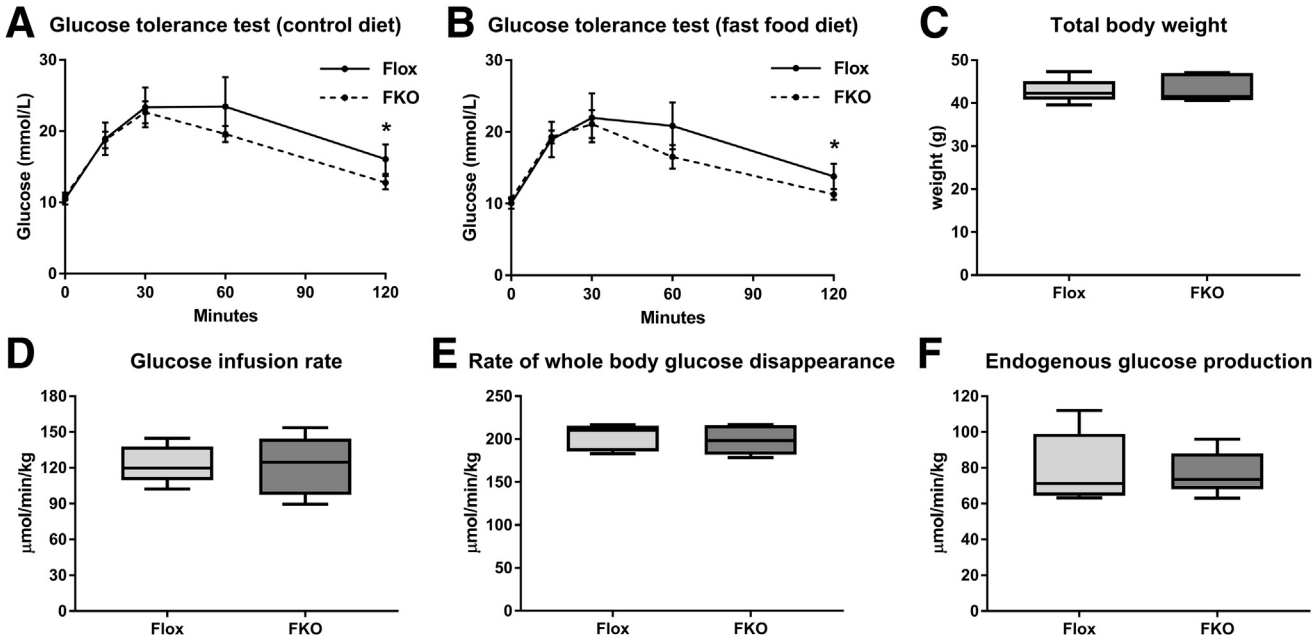

Figure 7. Adipocyte-specific ferroportin deletion does not influence glucose homeostasis. (*A* and *B*) Glucose tolerance tests at 0, 15, 30, 60, and 120 minutes. Means with 95% CIs. *$P < .05$ at a single time point (Student *t* test) (n = 8–12 per group). (*A*) Control diet. (*B*) Fast food diet. (*C–F*) Hyperinsulinemic–euglycemic clamp studies (n = 5 per group). Differences between Flox and FKO groups were all NS (Student *t* test). (*C*) Body weight. (*D*) Glucose infusion rate. (*E*) Rate of whole-body glucose disappearance. (*F*) Endogenous glucose production.

indicating that adipocyte-specific ferroportin knockout does not affect insulin resistance in this model.

We have shown reduced hepatic and splenic iron concentrations as a result of the fast food diet, suggesting reduced body iron stores as a consequence of a high-calorie diet. The hormone hepcidin is considered the key regulator of body iron homeostasis.[32] Hepcidin production is reported to be increased in individuals with NAFLD.[33] It therefore might be expected that low HIC in these mice could be explained by increased *Hamp1* expression leading to reduced intestinal iron absorption after the internalization of enterocyte ferroportin.[8] However, *Hamp1* expression was decreased markedly in these mice, suggesting appropriate *Hamp1* response to reduced hepatic iron stores and is consistent with previous studies.[25,34–36] These findings are also in keeping with the established association between iron deficiency and obesity in human beings.[37,38] Orr et al[34] showed that a high-fat diet led to iron repartitioning with a reduction in HIC and an increase in adipocyte iron concentration via an unknown mechanism, although this was not seen in our model.

Table 3. Increased Liver Injury With Fast Food Diet, but Not With *Fpn1* Deletion

	Control diet			Fast food diet		
	Flox	FKO	*P*	Flox	FKO	*P*
NAS (0–8)	4 (0–6)	2 (0–5)	NS	6 (5–7)	6 (5–7)	NS
Steatosis (0–3)	2.5 (0–3)	1.5 (0–3)	NS	3 (3–3)	3 (3–3)	NS
Lobular inflammation (0–3)	0 (0–1)	0 (0–1)	NS	1 (0–2)	1 (0–2)	NS
Ballooning (0–2)	1.5 (0–2)	0.5 (0–2)	NS	2 (2–2)	2 (2–2)	NS
Fibrosis (0–4)	0 (0–1)	0 (0–2)	NS	2 (1–2)	2 (2–2)	NS

NOTE. Median score (range) for NAS (score, 0–8), macrovesicular steatosis (grade, 0–3), lobular inflammation (grade, 0–3), ballooning (grade, 0–2), fibrosis (grade, 0–4). *P* value was the result of Mann–Whitney tests comparing genotypes for each diet (n = 8–12 per group).
NAS, NAFLD activity score.

The fast food diet model involves 5 months of exposure to a high-calorie diet and high-fructose corn syrup in drinking water in mice housed singly to mimic a sedentary lifestyle.[22] We have found this to be a reliable model for the generation of a phenotype of steatohepatitis and hepatic fibrosis as shown by expert histologic assessment and supported further by quantification of Oil Red O, heme oxygenase 1 mRNA, and hepatic hydroxyproline. Furthermore, the high residual endogenous glucose production during hyperinsulinemic clamp studies suggests profound insulin resistance in this model, which is a highly appropriate feature for a model of human NASH. It was unexpected, however, that our mice fed a control diet should develop significant amounts of simple steatosis. This may be explained in part by a number of factors including single housing leading to a sedentary existence and a relatively advanced age of the mice.

Adipose tissue macrophage infiltration is a hallmark of obesity and steatohepatitis in human beings.[5,39] We have shown that the fast food diet model generates a significant

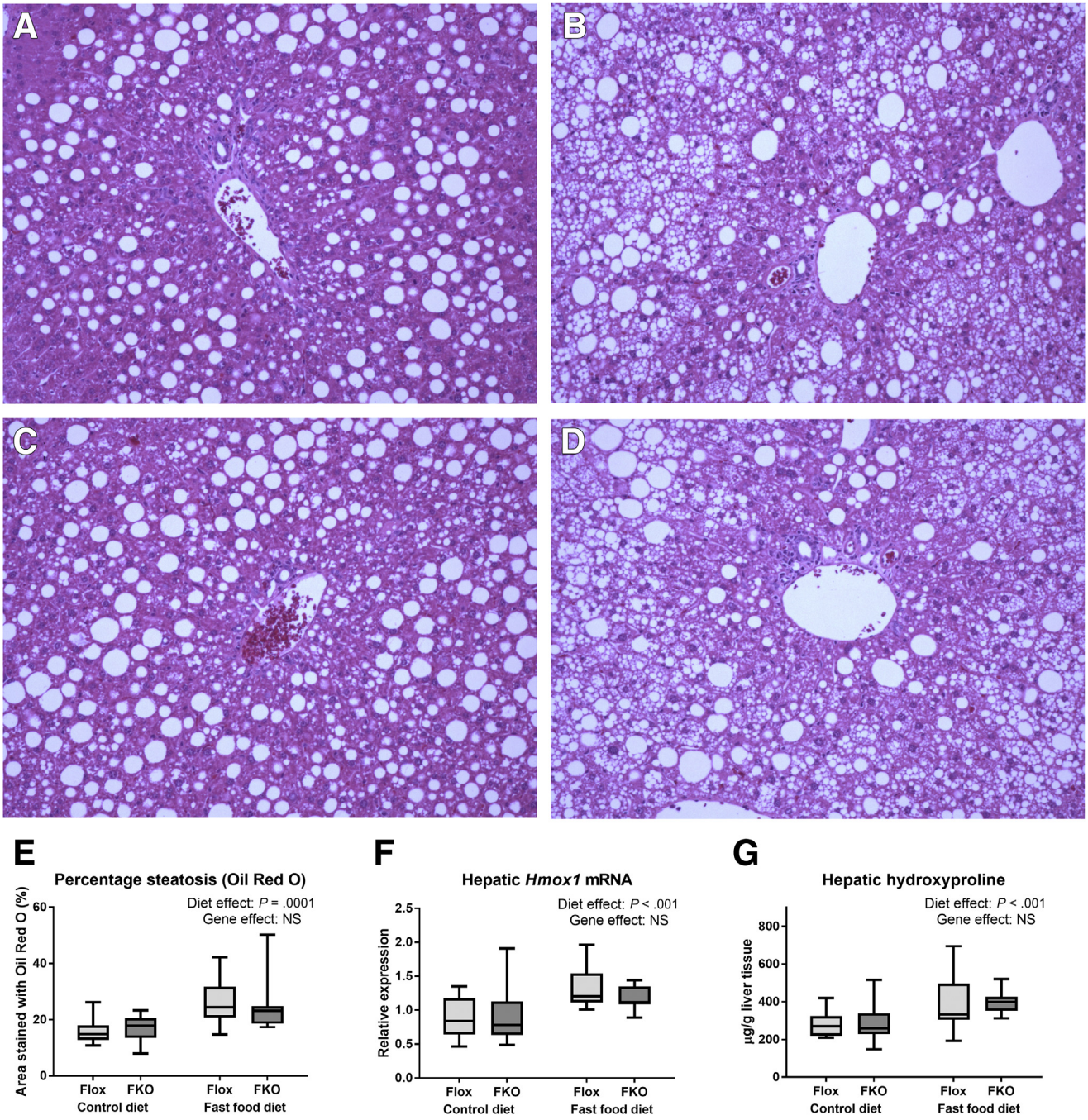

Figure 8. Fast food diet, but not genotype, leads to steatohepatitis. (*A–D*) Light microscopy of representative liver sections stained with H&E. *Original magnification*: ×200. (*A*) Flox control diet. (*B*) Flox fast food diet. (*C*) FKO control diet. (*D*) FKO fast food diet. (*E*) Percentage area of liver sections stained with Oil Red O. Oil Red O staining was increased by the fast food diet ($P = .0001$), but unaltered by genotype (NS, both 2-way ANOVA). (*F*) Liver heme oxygenase 1 (*Hmox1*) mRNA. The fast food diet led to increased Hmox1 mRNA ($P < .001$), but there was no genotype effect (NS, 2-way ANOVA). (*G*) Hepatic hydroxyproline. Hydroxyproline was increased by the fast food diet ($P < .001$), but was unaffected by genotype (NS, 2-way ANOVA) (n = 8–12 per group).

increase in adipose tissue macrophage infiltration with crown-like structures. This further validates the applicability of the fast food diet model for use in the study of NASH. We had considered that an increase in adipocyte iron in FKO mice might create an inflammatory state induced by oxidative stress and lead to macrophage infiltration. However, given the observed lack of effect of FKO on iron phenotype, it seems unsurprising that genotype did not affect macrophage infiltration in this model. In our study, we found that EFP weight was lower in FKO mice, although this was seen only in animals fed the control and not the fast food diet. In the context of unaltered iron phenotype and

lack of effect in fast food diet–fed mice, the significance of this result remains uncertain. When we studied adipokine expression in our model, we found increased adipocyte *leptin* mRNA and decreased *RBP-4* mRNA with a fast food diet. These findings are broadly consistent with human studies of NASH, although conflicting reports exist in the literature.[7,40,41]

In summary, our findings indicate that the physiological role of ferroportin in adipocytes may be limited and other factors involved in iron homeostasis may be more important in these cells. Because adipocyte iron appears to play a key role in physiological processes, such as appetite regulation, and pathophysiological processes, such as NAFLD and diabetes, a greater understanding of iron metabolism in these cells is clearly a target for future studies.

References

1. Loomba R, Sanyal AJ. The global NAFLD epidemic. Nat Rev Gastroenterol Hepatol 2013;10:686–690.
2. Anstee QM, Targher G, Day CP. Progression of NAFLD to diabetes mellitus, cardiovascular disease or cirrhosis. Nat Rev Gastroenterol Hepatol 2013;10:330–344.
3. Vernon G, Baranova A, Younossi ZM. Systematic review: the epidemiology and natural history of non-alcoholic fatty liver disease and non-alcoholic steatohepatitis in adults. Aliment Pharmacol Ther 2011;34:274–285.
4. Khan FZ, Perumpail RB, Wong RJ, Ahmed A. Advances in hepatocellular carcinoma: nonalcoholic steatohepatitis-related hepatocellular carcinoma. World J Hepatol 2015;7:2155–2161.
5. Hebbard L, George J. Animal models of nonalcoholic fatty liver disease. Nat Rev Gastroenterol Hepatol 2011; 8:35–44.
6. Donnelly KL, Smith CI, Schwarzenberg SJ, Jessurun J, Boldt MD, Parks EJ. Sources of fatty acids stored in liver and secreted via lipoproteins in patients with nonalcoholic fatty liver disease. J Clin Invest 2005; 115:1343–1351.
7. Marra F, Bertolani C. Adipokines in liver diseases. Hepatology 2009;50:957–969.
8. Anderson GJ, Vulpe CD. Mammalian iron transport. Cell Mol Life Sci 2009;66:3241–3261.
9. Gabrielsen JS, Gao Y, Simcox JA, Huang J, Thorup D, Jones D, Cooksey RC, Gabrielsen D, Adams TD, Hunt SC, Hopkins PN, Cefalu WT, McClain DA. Adipocyte iron regulates adiponectin and insulin sensitivity. J Clin Invest 2012;122:3529–3540.
10. Pihan-Le Bars F, Bonnet F, Loreal O, Le Loupp AG, Ropert M, Letessier E, Prieur X, Bach K, Deugnier Y, Fromenty B, Cariou B. Indicators of iron status are correlated with adiponectin expression in adipose tissue of patients with morbid obesity. Diabetes Metab 2016; 42:105–111.
11. Bekri S, Gual P, Anty R, Luciani N, Dahman M, Ramesh B, Iannelli A, Staccini-Myx A, Casanova D, Ben Amor I, Saint-Paul MC, Huet PM, Sadoul JL, Gugenheim J, Srai SK, Tran A, Le Marchand-Brustel Y. Increased adipose tissue expression of hepcidin in severe obesity is independent from diabetes and NASH. Gastroenterology 2006;131:788–796.
12. Simcox JA, McClain DA. Iron and diabetes risk. Cell Metab 2013;17:329–341.
13. Dongiovanni P, Fracanzani AL, Fargion S, Valenti L. Iron in fatty liver and in the metabolic syndrome: a promising therapeutic target. J Hepatol 2011;55:920–932.
14. Gao Y, Li Z, Gabrielsen JS, Simcox JA, Lee SH, Jones D, Cooksey B, Stoddard G, Cefalu WT, McClain DA. Adipocyte iron regulates leptin and food intake. J Clin Invest 2015;125:3681–3691.
15. Dongiovanni P, Ruscica M, Rametta R, Recalcati S, Steffani L, Gatti S, Girelli D, Cairo G, Magni P, Fargion S, Valenti L. Dietary iron overload induces visceral adipose tissue insulin resistance. Am J Pathol 2013; 182:2254–2263.
16. Fernandez-Real JM, Moreno JM, Ricart W. Circulating retinol-binding protein-4 concentration might reflect insulin resistance-associated iron overload. Diabetes 2008;57:1918–1925.
17. Green A, Basile R, Rumberger JM. Transferrin and iron induce insulin resistance of glucose transport in adipocytes. Metabolism 2006;55:1042–1045.
18. Casey JL, Hentze MW, Koeller DM, Caughman SW, Rouault TA, Klausner RD, Harford JB. Iron-responsive elements: regulatory RNA sequences that control mRNA levels and translation. Science 1988;240:924–928.
19. Wang ZV, Deng Y, Wang QA, Sun K, Scherer PE. Identification and characterization of a promoter cassette conferring adipocyte-specific gene expression. Endocrinology 2010;151:2933–2939.
20. Eguchi J, Wang X, Yu S, Kershaw EE, Chiu PC, Dushay J, Estall JL, Klein U, Maratos-Flier E, Rosen ED. Transcriptional control of adipose lipid handling by IRF4. Cell Metab 2011;13:249–259.
21. Lee KY, Russell SJ, Ussar S, Boucher J, Vernochet C, Mori MA, Smyth G, Rourk M, Cederquist C, Rosen ED, Kahn BB, Kahn CR. Lessons on conditional gene targeting in mouse adipose tissue. Diabetes 2013; 62:864–874.
22. Charlton M, Krishnan A, Viker K, Sanderson S, Cazanave S, McConico A, Masuoko H, Gores G. Fast food diet mouse: novel small animal model of NASH with ballooning, progressive fibrosis, and high physiological fidelity to the human condition. Am J Physiol Gastrointest Liver Physiol 2011;301:G825–G834.
23. Donovan A, Lima CA, Pinkus JL, Pinkus GS, Zon LI, Robine S, Andrews NC. The iron exporter ferroportin/Slc40a1 is essential for iron homeostasis. Cell Metab 2005;1:191–200.
24. Brunt EM. Nonalcoholic fatty liver disease: what the pathologist can tell the clinician. Dig Dis 2012;30(Suppl 1):61–68.
25. Britton L, Jaskowski L, Bridle K, Santrampurwala N, Reiling J, Musgrave N, Subramaniam VN, Crawford D. Heterozygous Hfe gene deletion leads to impaired glucose homeostasis, but not liver injury in mice fed a high-calorie diet. Physiol Rep 2016;4:12.
26. Xirouchaki CE, Mangiafico SP, Bate K, Ruan Z, Huang AM, Tedjosiswoyo BW, Lamont B, Pong W,

Favaloro J, Blair AR, Zajac JD, Proietto J, Andrikopoulos S. Impaired glucose metabolism and exercise capacity with muscle-specific glycogen synthase 1 (gys1) deletion in adult mice. Mol Metab 2016;5:221–232.
27. Kleiner DE, Brunt EM, Van NM, Behling C, Contos MJ, Cummings OW, Ferrell LD, Liu YC, Torbenson MS, Unalp-Arida A, Yeh M, McCullough AJ, Sanyal AJ. Design and validation of a histological scoring system for nonalcoholic fatty liver disease. Hepatology 2005; 41:1313–1321.
28. Bridle KR, Sobbe AL, de Guzman CE, Santrampurwala N, Jaskowski LA, Clouston AD, Campbell CM, Nathan Subramaniam V, Crawford DH. Lack of efficacy of mTOR inhibitors and ACE pathway inhibitors as antifibrotic agents in evolving and established fibrosis in Mdr2(-)/(-) mice. Liver Int 2015;35:1451–1463.
29. Fleming RE, Ponka P. Iron overload in human disease. N Engl J Med 2012;366:348–359.
30. Cinti S, Mitchell G, Barbatelli G, Murano I, Ceresi E, Faloia E, Wang S, Fortier M, Greenberg AS, Obin MS. Adipocyte death defines macrophage localization and function in adipose tissue of obese mice and humans. J Lipid Res 2005;46:2347–2355.
31. Lickteig AJ, Fisher CD, Augustine LM, Cherrington NJ. Genes of the antioxidant response undergo upregulation in a rodent model of nonalcoholic steatohepatitis. J Biochem Mol Toxicol 2007;21:216–220.
32. Rishi G, Wallace DF, Subramaniam VN. Hepcidin: regulation of the master iron regulator. Biosci Rep 2015; 35:3.
33. Kroot JJ, Tjalsma H, Fleming RE, Swinkels DW. Hepcidin in human iron disorders: diagnostic implications. Clin Chem 2011;57:1650–1669.
34. Orr JS, Kennedy A, Anderson-Baucum EK, Webb CD, Fordahl SC, Erikson KM, Zhang Y, Etzerodt A, Moestrup SK, Hasty AH. Obesity alters adipose tissue macrophage iron content and tissue iron distribution. Diabetes 2014;63:421–432.
35. Chung J, Kim MS, Han SN. Diet-induced obesity leads to decreased hepatic iron storage in mice. Nutr Res 2011; 31:915–921.
36. Sonnweber T, Ress C, Nairz M, Theurl I, Schroll A, Murphy AT, Wroblewski V, Witcher DR, Moser P, Ebenbichler CF, Kaser S, Weiss G. High-fat diet causes iron deficiency via hepcidin-independent reduction of duodenal iron absorption. J Nutr Biochem 2012; 23:1600–1608.
37. Coimbra S, Catarino C, Santos-Silva A. The role of adipocytes in the modulation of iron metabolism in obesity. Obes Rev 2013;14:771–779.
38. Siddique A, Nelson JE, Aouizerat B, Yeh MM, Kowdley KV, Network NCR. Iron deficiency in patients with nonalcoholic fatty liver disease is associated with obesity, female gender, and low serum hepcidin. Clin Gastroenterol Hepatol 2014;12:1170–1178.
39. Weisberg SP, McCann D, Desai M, Rosenbaum M, Leibel RL, Ferrante AW Jr. Obesity is associated with macrophage accumulation in adipose tissue. J Clin Invest 2003;112:1796–1808.
40. Wolfs MG, Gruben N, Rensen SS, Verdam FJ, Greve JW, Driessen A, Wijmenga C, Buurman WA, Franke L, Scheja L, Koonen DP, Shiri-Sverdlov R, van Haeften TW, Hofker MH, Fu J. Determining the association between adipokine expression in multiple tissues and phenotypic features of non-alcoholic fatty liver disease in obesity. Nutr Diabetes 2015;5:e146.
41. Alkhouri N, Lopez R, Berk M, Feldstein AE. Serum retinol-binding protein 4 levels in patients with nonalcoholic fatty liver disease. J Clin Gastroenterol 2009; 43:985–989.

Received September 13, 2017. Accepted January 3, 2018.

Correspondence
Address correspondence to: Laurence Britton, MBChB, FRACP, Gallipoli Medical Research Institute, Greenslopes Private Hospital, Newdegate Street, Greenslopes, Queensland, 4120, Australia. e-mail: l.britton@uq.edu.au; fax: (61) 7-3394-7767.

Acknowledgments
The authors would like to thank Barbara Matthews at Pathology Queensland Central Laboratory, Herston, Queensland, Australia, who performed the adipocyte iron assays.

Author contributions
Laurence Britton was responsible for the study concept and design, acquisition of data, analysis and interpretation of data, drafting of the manuscript, and statistical analysis; Lesley-Anne Jaskowski was responsible for the acquisition of data, analysis and interpretation of data, critical revision of the manuscript for important intellectual content, and technical support; Kim Bridle was responsible for the study concept and design, analysis and interpretation of data, critical revision of the manuscript for important intellectual content, and study supervision; Eriza Secondes was responsible for the acquisition of data and technical support; Daniel Wallace was responsible for the study concept and design, analysis and interpretation of data, and critical revision of the manuscript for important intellectual content; Nishreen Santrampurwala was responsible for the study concept and design, analysis and interpretation of data, and critical revision of the manuscript for important intellectual content; Janske Reiling was responsible for the study concept and design, analysis and interpretation of data, and critical revision of the manuscript for important intellectual content; Gregory Miller was responsible for the analysis and interpretation of data, drafting of the manuscript, and critical revision of the manuscript for important intellectual content; Salvatore Mangiafico was responsible for the study concept and design, acquisition of data, analysis and interpretation of data, drafting of the manuscript, and critical revision of the manuscript for important intellectual content; Sofianos Andrikopoulos was responsible for the study concept and design, analysis and interpretation of data, critical revision of the manuscript for important intellectual content, and material support; V. Nathan Subramaniam was responsible for the study concept and design, analysis and interpretation of data, critical revision of the manuscript for important intellectual content, material support, and study supervision; and Darrell Crawford was responsible for the study concept and design, analysis and interpretation of data, critical revision of the manuscript for important intellectual content, statistical analysis, material support, and study supervision.

Conflicts of interest
The authors disclose no conflicts.

Funding
Supported by funding from the National Health and Medical Research Council (APP1029574); and by scholarships from the Gallipoli Medical Research Foundation and the Gastroenterological Society of Australia (L.B.).